Published in final edited form as:
J Biomol Screen. 2009 December ; 14(10): 1195–1206. doi:10.1177/1087057109347473.

Two $G\alpha_{i1}$ Rate-Modifying Mutations Act in Concert to Allow Receptor-Independent, Steady-State Measurements of RGS Protein Activity

THOMAS ZIELINSKI[1,§], **ADAM J. KIMPLE**[2,§], **STEPHANIE Q. HUTSELL**[3], **MARK D. KOEFF**[1], **DAVID P. SIDEROVSKI**[2,4,5], and **ROBERT G. LOWERY**[1]

[1]BellBrook Labs 5500 Nobel Drive, Suite 250, Madison, WI 53711

[2]Department of Pharmacology, The University of North Carolina at Chapel Hill, Chapel Hill, NC 27599-7365

[3]Department of Biochemistry & Biophysics, The University of North Carolina at Chapel Hill, Chapel Hill, NC 27599-7365

[4]Lineberger Comprehensive Cancer Center, The University of North Carolina at Chapel Hill, Chapel Hill, NC 27599-7365

[5]UNC Neuroscience Center, The University of North Carolina at Chapel Hill, Chapel Hill, NC 27599-7365

Abstract

RGS proteins are critical modulators of G protein-coupled receptor (GPCR) signaling given their ability to deactivate Gα subunits via “GTPase-accelerating protein” (GAP) activity. Their selectivity for specific GPCRs makes them attractive therapeutic targets. However, measuring GAP activity is complicated by slow GDP release from Gα and lack of solution-phase assays for detecting free GDP in the presence of excess GTP. To overcome these hurdles, we developed a $G\alpha_{i1}$ mutant with increased GDP dissociation and decreased GTP hydrolysis, enabling detection of GAP activity using steady-state GTP hydrolysis. $G\alpha_{i1}$(R178M/A326S) GTPase activity was stimulated 6~12 fold by RGS proteins known to act on $G\alpha_i$ subunits, and not affected by those unable to act on $G\alpha_i$, demonstrating that the Gα/RGS domain interaction selectivity was not altered by mutation. $G\alpha_{i1}$(R178M/A326S) interacted with RGS proteins with expected binding specificity and affinities. To enable non-radioactive, homogenous detection of RGS protein effects on $G\alpha_{i1}$(R178M/A326S), we developed a Transcreener® fluorescence polarization immunoassay based on a monoclonal antibody that recognizes GDP with greater than 100-fold selectivity over GTP. Combining $G\alpha_{i1}$(R178M/A326S) with a homogenous, fluorescence-based GDP detection assay provides a facile means to explore the targeting of RGS proteins as a new approach for selective modulation of GPCR signaling.

Keywords

Fluorescence polarization; GDP detection; regulators of G-protein signaling; surface plasmon resonance

Address correspondence to: David P. Siderovski, PhD, UNC-Chapel Hill, 4073 Genetics Medicine Bldg, 120 Mason Farm Road, CB#7365, Chapel Hill, NC 27599-7365. Tel: 919-843-9363 Fax: 919-966-5640 dsiderov@med.unc.edu;. Robert G. Lowery, PhD, BellBrook Labs, 5500 Nobel Drive, Suite 250, Madison, WI 53711. Tel: 608-227-4501 Fax: 608-441-2967 bob.lowery@bellbrooklabs.com..

[§]T.Z. and A.J.K. are co-first authors who contributed equally to this work.

INTRODUCTION

The standard model of GPCR signal transduction had long been restricted to a three-component system: receptor, G-protein, and effector 1. The seven-transmembrane domain receptor is coupled to a membrane-associated heterotrimeric complex composed of a GTP-hydrolyzing Gα subunit and a Gβγ dimeric partner. Agonist-induced conformational changes enhance the guanine nucleotide exchange activity of the receptor, leading to the release of GDP (and subsequent binding of GTP) by the Gα subunit. On binding GTP, conformational changes within the three `switch' regions of Gα allow the release of Gβγ. Separated Gα·GTP and Gβγ subunits are then free to propagate intracellular signaling via diverse effectors 2. The intrinsic GTP hydrolysis (GTPase) activity of Gα resets the cycle by forming Gα·GDP which has low affinity for effectors but high affinity for Gβγ. In this way, the inactive, GDP-bound heterotrimer (Gα·GDP/Gβγ) is reformed and capable once again to interact with activated receptor.

Based on this cycle of receptor-catalyzed GTP exchange and intrinsic GTP hydrolysis by Gα, the duration of heterotrimeric G-protein signaling is thought to be controlled by the lifetime of the Gα subunit in its GTP-bound state. After the establishment of this basic model 1, RGS proteins ("regulators of G-protein signaling") were subsequently discovered 3⁻5 to bind Gα subunits (via a conserved ~120 amino-acid RGS domain) and dramatically accelerate their intrinsic GTPase activity 6, thereby attenuating heterotrimer-linked signaling. Nearly 40 human proteins contain at least one RGS domain, with many of these proteins (*e.g.*, RGS4, RGS16) serving as GTPase-accelerating proteins (GAPs) for $G\alpha_{i/o}$ subunits, yet others such as RGS2 and p115-RhoGEF being particularly attuned to $G\alpha_{q/11}$ and $G\alpha_{12/13}$ substrates, respectively 7 . The discovery of this superfamily of Gα-directed GAPs resolved apparent timing paradoxes between observed rapid physiological responses mediated by GPCRs and the slow hydrolysis activity of the cognate G-proteins seen *in vitro*. Thus, in this capacity as negative regulators of GPCR signal transduction, the RGS proteins present themselves as excellent potential drug discovery targets 7. For example, pharmacological inhibition of RGS domain GAP activity should lead to prolonged signaling from G-proteins activated by agonist-bound GPCRs.

The most direct way to detect RGS protein function is by measuring the increased GTPase activity exhibited by its target Gα protein. However, accurate *in vitro* measurements of Gα-catalyzed GTP hydrolysis are difficult to obtain without laborious biochemical reconstitutions with purified Gβγ and an activated GPCR (*e.g.*, ref. 8). In the absence of GPCR-mediated nucleotide exchange, it is GDP release (rather than GTP hydrolysis) that is the rate-limiting step in the Gα nucleotide cycle 9. Thus, to examine the effect of an RGS protein in accelerating GTP hydrolysis by an isolated Gα subunit *in vitro*, a single round of hydrolysis of radiolabelled GTP is usually performed (*a.k.a.* the "single-turnover GTPase assay"; ref. 6). This standard assay for measuring RGS domain-mediated GAP activity is low-throughput and requires discrete steps of [γ-^{32}P]GTP loading onto Gα, protein reactant admixture (with addition of the critical cofactor Mg^{2+} to initiate hydrolysis), isolation (in discrete time intervals) of released [^{32}P]phosphate with activated charcoal precipitation and centrifugation, and finally scintillation counting. We have described an alternative single-turnover GTPase assay 10 using a coumarin-labeled, phosphate-binding protein to facilitate fluorescence-based detection of inorganic phosphate production; however, this method demands stringent controls on multiple experimental steps to eliminate phosphate contaminants that interfere with the detection of GTPase activity. Such convoluted protocols of inorganic phosphate detection are difficult for the non-specialist and especially not suited for high-throughput screening (HTS) of large compound libraries for RGS domain inhibitors. We and others have reported alternative, fluorescence-based strategies for detecting the binding between RGS protein and Gα substrate 11⁻13, but none has

specifically facilitated a discrete endpoint measurement of RGS domain-mediated GAP activity *per se*.

In order to develop a facile steady-state GTPase assay for RGS domain GAP activity, we first set out to increase the spontaneous GDP release rate of Gα ($k_{off(GDP)}$) while also decreasing its intrinsic rate of GTP hydrolysis ($k_{cat(GTPase)}$), thereby allowing detection of at least a five-fold enhancement of steady-state GTP hydrolysis by RGS proteins to provide an adequate signal-to-noise ratio. $G\alpha_{i1}$ and closely related Gα proteins have been the focus of extensive structure/function studies 14–17, and point mutations that affect both $k_{off(GDP)}$ and $k_{cat(GTPase)}$ without affecting functional interaction with the RGS domain have been identified previously 15–18 (*e.g.*, Fig. 1A). Two of the most striking Gα mutations have been made to the highly-conserved active-site arginine (R178C; ref. 15), which causes a ~100-fold reduction in GTPase activity, and to the alanine residue within the conserved TCAT loop that contacts the guanine ring (A326S; ref. 16), which results in a ~25-fold increase in $k_{off(GDP)}$ relative to wildtype yet an identical $k_{cat(GTPase)}$.

To detect RGS protein-accelerated GTPase activity, we adapted a monoclonal antibody and fluorescent tracer, previously developed for the Transcreener ADP assay 19, for selective immunodetection of GDP with a fluorescence polarization readout. Measurement of GTPase activity using this Transcreener GDP assay overcomes the signal-to-noise limitations of phosphate detection methods and has been validated as a robust HTS method in the case of ADP detection for kinases and ATPases 20–22. Moreover, because it is a catalytic assay rather than a substrate binding assay, it should enable detection of all types of modulators of RGS protein GAP activity, including those that bind at allosteric sites and affect RGS protein catalytic activity without directly targeting the RGS domain Gα binding-site 23.

In this present study, we tested multiple point-mutant $G\alpha_{i1}$ proteins with increased GDP dissociation and/or decreased GTP hydrolysis rates for their ability to enable detection of RGS domain GAP activity using a steady-state GTPase assay format (*i.e.*, multiple rounds of turnover of GTP to GDP). Coupling one of these variants, $G\alpha_{i1}$(R178M/A326S), to the Transcreener GDP detection system has not only allowed facile detection of RGS protein GAP activity, but was useful in helping establish (along with surface plasmon resonance spectroscopy) that the mutant $G\alpha_{i1}$ interacted with RGS proteins with the same specificity and affinity as the wildtype $G\alpha_{i1}$ protein.

MATERIALS AND METHODS

Chemicals and assay materials

GDP and GTP were purchased from USB Corp. (Cleveland, OH). The monoclonal antibody and tracer used for GDP detection were developed at BellBrook Labs (Madison, WI) as described 19, with the tracer comprising ADP conjugated to Alexa Fluor 633 (Invitrogen/ Molecular Probes). Unless otherwise specified, all additional reagents were of the highest quality obtainable from Sigma (St. Louis, MO) or Fisher Scientific (Hampton, NH).

Protein expression and purification

Wildtype, full-length human $G\alpha_{i1}$ and various RGS proteins used in these studies were expressed in *E. coli* and purified as previously described 24. $G\alpha_{i1}$ point mutants were created using PCR-based site-directed mutagenesis (QuikChange® II, Stratagene; La Jolla, CA) on the wildtype pProEXHTb-$G\alpha_{i1}$ expression vector; mutagenesis primers were designed using Stratagene's QuikChange primer-design program and synthesized/PAGE-purified by Sigma-Genosys. All mutant constructs were sequence verified at Functional Biosciences LLC (Madison, WI) before protein expression, purification, concentration, quantitation, and cryopreservation using established protocols 10,24.

Radiolabeled nucleotide binding and single turnover GTPase assays

Assessments of spontaneous GDP release and single-turnover GTP hydrolysis rates by wildtype and mutant $G\alpha_{i1}$ subunits, using measurements of [^{35}S]GTPγS binding and [γ-^{32}P]GTP hydrolysis respectively, were conducted exactly as previously described 24,25. Briefly, for [^{35}S]GTPγS binding by 100 nM of $G\alpha_{i1}$ subunits at 20 °C, timed aliquots were removed, filtered through nitrocellulose, and washed four times with 10 ml of wash buffer before scintillation counting. Assays were conducted in duplicate, counts were subtracted from analogous reactions in "non-specific binding" buffer 24, and normalized data plotted as mean ± S.E.M. For single-turnover [γ-^{32}P]GTP hydrolysis assays, $G\alpha_{i1}$ subunits (100 nM) were pre-bound to [γ-^{32}P]GTP in the absence of Mg^{2+} for 10 minutes at 30 °C. Reactions were then initiated by the addition of 10 mM $MgCl_2$ (final concentration) and the production of $^{32}P_i$ was measured by activated charcoal filtration and liquid scintillation counting 9,25. Initial rates obtained by data analysis using GraphPad Prism (La Jolla, CA).

Radiolabeled nucleotide steady-state GTPase assays

Assessments of steady-state [γ-^{32}P]GTP hydrolysis rates by wildtype and mutant $G\alpha_{i1}$ subunits were conducted essentially as previously described 26. Briefly, $G\alpha_{i1}$ protein was diluted to 50 nM in a buffer containing 50 mM Tris pH 7.5, 100 mM NaCl, 0.05% $C_{12}E_{10}$, 1 mM DTT, 5 mM EDTA, 10 mM $MgCl_2$, and 5 μg/ml BSA. Assays were initiated with the addition of [γ-^{32}P]GTP (and RGS4 if used), aliquots stopped at indicated time intervals, and free [γ-^{32}P]Pi quantified as previously described 26.

Transcreener GDP assays

Standard curves and GTPase reactions were both run at 30 °C in kinetic mode on a Tecan Safire2 multiwell reader in Corning® 384-well black round-bottom low-volume polystyrene non-binding surface microplates (Part # 3676). Fluorescence polarization was read using 635 nm excitation (20 flashes per well) and 670 nm emission. A free tracer reference was set to 20 mP by adjusting the photomultiplier tubes, and buffer containing GDP antibody alone was used as a blank for sample and reference wells. EC_{50} and EC_{85} values, Hill slopes, and curves were generated by GraphPad Prism (La Jolla, CA). Unless otherwise indicated, reactions were run in 20 mM Tris 7.5 pH, 1 mM EDTA, 10 mM $MgCl_2$, 10 μM GTP, 8 μg/ml GDP antibody, and 2 nM tracer in a final 20 μl volume. GDP antibody was used at a concentration 85% of the amount required for saturated binding to tracer (*i.e.*, the EC_{85}). Where shown, polarization data was converted to the amount of GDP produced using standard curves. Reaction rates were then determined in GraphPad Prism using linear regression to estimate slope. For GTPase and GAP assays, reactions were started with the addition of GTP with or without RGS protein.

Compound interference test

To assess the robustness of the Transcreener GDP assay for practical screening applications, we performed a control screen using the GenPlus library of 960 bioactive molecules from Microsource Discovery Systems, many of which are approved drugs. GDP assay reagents (as denoted above) were added to duplicate wells containing 10 μM compound and either 10 μM GTP to mimic no-enzyme control reactions or 9 μM GTP plus 1 μM GDP to mimic completed enzyme reactions in 1% DMSO.

Pilot screen and counterscreen of GenPlus Library

Screens of the GenPlus library with the Transcreener GDP assay (10 μM final compound concentration) for modulators of RGS4 GAP activity on $G\alpha_{i1}$(R178M/A326S), as well as for non-specific modulators of intrinsic GTPase activity of $G\alpha_{i1}$(R178M/A326S) alone, were conducted as mentioned above with the following changes. GTPase reactions containing 50

nM $G\alpha_{i1}$(R178M/A326S) with or without 250 nM RGS4 were run in Corning® 384-well microplates at 30 °C in 20 mM Tris pH 7.5, 1 mM EDTA, 10 mM $MgCl_2$, 10 μM GTP, 12 μg/μl GDP antibody, 2 nM tracer, and 0.5% DMSO (v/v) in a final volume of 20 μl. Fluorescence polarization was read at 60, 90, 120, and 180 minutes of elapsed reaction time on a Tecan Safire2 multiwell reader as described above.

Surface plasmon resonance (SPR) spectroscopy

Optical detection of surface plasmon resonance (SPR) was performed using a BIAcore 3000 (GE Healthcare; Piscataway, NJ). Wildtype and mutant $G\alpha_{i1}$ proteins were immobilized onto nickel-nitrilotriacetic acid SPR sensor chips (GE Healthcare) by hexahistidine tag-mediated capture-coupling as previously described 27. Affinities of RGS proteins for immobilized $G\alpha_{i1}$ proteins were obtained from dose-response sensorgrams using equilibrium saturation binding analyses as previously described 24.

RESULTS AND DISCUSSION

Profiling multiple $G\alpha_{i1}$ point-mutations for nucleotide cycling rate alterations

Using PCR-based site-directed mutagenesis, we created several amino-acid substitutions at various positions within $G\alpha_{i1}$ known to affect $k_{off(GDP)}$ and/or $k_{cat(GTPase)}$ (*e.g.*, Fig. 1). These mutants included: aspartate, serine, or threonine replacing Ala-326; cysteine, lysine, or methionine replacing Arg-178; alanine, serine, or valine replacing Thr-181; single mutants K192A and F336A; and double mutants K192A/F336A, R178C/A326S, R178C/A326T, R178M/A326S, R178C/A326T, and T181A/A326S. Note that multiple different substitutions were made at several sites, including amino-acids intended to be more or less disruptive than the original reported mutation. For instance, R178K and R178M were tested as more conservative substitutions at the catalytic arginine position relative to the original R178C variant; it was thought that either of these alternative substitutions might result in a smaller decrease in $k_{cat(GTPase)}$ than the cysteine replacement which reduces $k_{cat(GTPase)}$ by two orders of magnitude 15. While the R178C mutation leads to a substantial decrease in $k_{cat(GTPase)}$, Berman *et al.* 6 have shown that the single-turnover GTPase rate of this Gα mutant can still be increased by RGS domain-mediated GAP activity, whereas the more conventional GTPase-crippling mutation of Q204L renders $G\alpha_{i1}$ truly dead in terms of responsiveness to RGS proteins. Thus, the $G\alpha_{i1}$(Q204L) mutant was not pursued in this study.

$G\alpha_{i1}$ mutants were initially profiled for enhanced GDP release and/or reduced GTPase rate sufficient to see a change in steady-state GTP hydrolysis upon RGS protein addition. This initial profiling led us to focus on two positions: Arg-178 and Ala-326. Binding of the non-hydrolyzable GTP analog, [^{35}S]GTPγS, to $G\alpha_{i1}$·GDP was used to measure the rate of GDP dissociation (*e.g.*, Fig. 1B); the prevailing assumption for Gα subunits is that k_{on} for [^{35}S]GTPγS binding is much more rapid than $k_{off(GDP)}$ 28. Single turnover GTP hydrolysis measuring $^{32}P_i$released from Gα-bound [γ-^{32}P]GTP – an assay format which is not rate-limited by GDP dissociation 9 – was used to assess intrinsic k_{cat} rates for the $G\alpha_{i1}$ mutants (*e.g.*, Figure 1C).

As expected, $G\alpha_{i1}$ variants with mutation to the active-site catalytic residue Arg-178 had very low or undetectable levels of GTP hydrolysis, whereas $G\alpha_{i1}$(A326S), the single mutation reported to only affect GDP dissociation, had a GTPase rate similar to wildtype $G\alpha_{i1}$ (Fig. 1C–D). [^{35}S]GTPγS binding assays showed that two variants with mutations only at the catalytic site, R178M and R178C, had GDP dissociation rates similar to wildtype $G\alpha_{i1}$, whereas introduction of the A326S mutation, either alone or in combination with R178C, caused a three-fold acceleration in GDP dissociation (Fig. 1B,D). When the A326S mutation was combined with methionine at Arg-178 (instead of cysteine), the GDP

dissociation rate increased more than ten-fold over wildtype: from 0.008 min^{-1} to 0.130 min^{-1} (Fig. 1D). We currently do not have a precise structural explanation for why the particular combination of R178M and A326S mutations results in more rapid GDP release than the single A326S mutation alone; it is not an additive effect, since the singly-mutated $G\alpha_{i1}$(R178M) variant exhibits wildtype GDP dissociation (Fig. 1B). It is interesting to note that Posner and colleagues, when reporting the crystal structure of the $G\alpha_{i1}$(A326S) mutant 16, suggested the presence of an indirect interaction between the Arg-178 and Ser-326 residues (via contacts with nucleotide and Gly-45), thereby providing a possible mechanism for the functional interaction we have observed here between the R178M and A326S mutations.

Combined action of two $G\alpha_{i1}$ mutations allows steady-state measurement of GAP activity

With the R178M/A326S mutant of $G\alpha_{i1}$ demonstrating the largest change in GDP release rate of all mutants tested, we next examined whether this particular $G\alpha_{i1}$ variant would be affected by RGS domain-mediated GAP activity in steady-state [γ-^{32}P]GTP hydrolysis assays. Addition of purified RGS4 protein to the $G\alpha_{i1}$(R178M/A326S) variant (in the presence of free [γ-^{32}P]GTP and Mg^{2+}) resulted in a dramatic increase in [^{32}P]Pi detected over time. In contrast, there was no effect of RGS4 on wildtype $G\alpha_{i1}$ in this steady-state assay (Fig. 2A *vs* B), as expected given the original report by Berman *et al.* 6.

Development of a Transcreener GDP assay

The Transcreener platform relies upon highly selective antibodies for detection of nucleotides produced in enzyme reactions 29. To allow measurement of RGS protein-mediated acceleration of steady-state GTP hydrolysis in a homogenous format without radioactivity, a Transcreener assay for GDP was developed (Figure 3A) using a competitive fluorescence polarization immunoassay format. For this method, a recently-developed monoclonal antibody that recognizes GDP with >100-fold higher affinity than GTP 19 is added to the reaction, along with a fluorescent tracer which binds to the antibody with high affinity. When no free, unlabeled GDP is present in the reaction, the fluorescent tracer remains antibody-bound and exhibits a high polarization given its high apparent molecular weight. GDP produced in the reaction displaces the tracer from the antibody, thereby reducing its apparent molecular weight, increasing its rotational motion, and thus reducing the degree of polarization of emitted light. A similar Transcreener assay has been widely used for detection of ADP produced by kinases and other ATP-hydrolyzing proteins (*e.g.*, refs. 20–22; reviewed in 29).

Figure 3B shows typical fluorescence polarization standard curves mimicking the conversion of GTP to GDP by a GTPase. An important aspect of flexibility for a GTPase assay is the ability to accommodate a range of initial GTP concentrations, so that diverse enzymes and screening strategies can be employed; therefore, these studies were performed using different GTP concentrations of 1, 10 and 100 μM. Because the antibody cross-reacts to some degree with GTP, its concentration must be increased as higher GTP concentrations are used, in order to buffer for the total guanine nucleotide pool. Thus, for this analysis, the EC_{85} concentrations of monoclonal antibody were first determined in the presence of the indicated initial GTP concentrations (2.2, 12 and 64 μg/ml Ab for 1, 10 and 100 μM GTP, respectively) and the standard curves for GTP to GDP conversion were performed with 16 replicates at those antibody concentrations. At a GDP concentration equivalent to 10% conversion of GTP, which is generally considered to be well within the initial velocity region, polarization shifts of 108, 134, and 148 mP were observed for the 1, 10, and 100 μM GTP concentration curves, respectively (Fig. 3B). Acceptable Z'-factor values (ref. 30) of greater than 0.5 were observed down to 2% conversion for the two higher initial GTP concentrations, and to 5% for the 1 μM initial GTP curve (Fig. 3C), suggesting that the

Transcreener GDP assay should be capable of very robust detection of GTPase enzyme initial velocity over at least a 100-fold range of initial GTP concentration.

To assess the potential for compound interference with the Transcreener GDP assay readout, we performed a control screen (Fig. 3D) with the GenPlus library of 960 bioactive molecules, many of which are approved drugs. This control screen was done under conditions mimicking 10% conversion to GDP for a GTPase reaction run at 10 μM initial GTP concentration. All wells were run in duplicate. The vast majority of the compounds clustered very tightly around the means for the 10 μM GTP and the 9 μM GTP/1 μM GDP conditions; the Z'-factor for the no-compound controls in this screen was 0.93. There were only three compounds in the control screen that caused the signal to vary more than three standard deviations from the mean: dirithromycin, metazolamide, and lonidamin (Figure 3D). There is no obvious structural similarity between them nor are any of them similar in structure to guanine nucleotide. These data suggests that compound interference with the Transcreener GDP assay readout will be minimal.

FP-based detection of RGS protein GAP activity is dependent on two rate-altering mutations

Having validated the utility of the Transcreener assay in detecting GDP in the presence of GTP, we next tested its use in measuring RGS protein GAP activity on several rate-altered $G\alpha_{i1}$ variants (Figure 4). In these experiments, the $G\alpha_{i1}$ proteins were incubated with and without the well-characterized, $G\alpha_i$-directed RGS protein RGS4 31 in the presence of the Transcreener GDP assay reagents, and plates were read at intervals starting at 15 minutes. The change in the absolute value of polarization at each time-point ($\Delta mP_t = | mP_t(G\alpha_{i1}) - mP_t(\text{no } G\alpha_{i1}) |$) was plotted over a time-course of 6 hours; in addition, the plotted change in polarization that occurred in the linear region (over the first hour) was converted to GDP formation using standard curves (akin to those of Figure 3B) and normalized to the amount of $G\alpha_{i1}$ protein present in the reaction, with the resultant initial rates of GTP hydrolysis calculated from these data shown in Fig. 4E.

The two $G\alpha_{i1}$ variants with single mutations at the catalytic arginine only, R178C or R178M, each had lower steady-state GTPase activity than wildtype $G\alpha_{i1}$ and, like wildtype, were unaffected by RGS4 (GAP factors of 0.9 and 1.2, respectively; Fig. 4E). These results are expected because their steady-state GTPase rate is limited by slow GDP dissociation. Conversely, the A326S variant exhibited a much higher steady-state GTPase rate than wildtype, as expected from its higher $k_{off(GDP)}$ (Fig. 1); however, its steady-state GTPase rate was unaffected by RGS4 (GAP ratio of 1.1; Fig. 4E), presumably because a further rate increase in GTPase is limited by k_{off}(GDP). Most importantly, the two double mutants, R178C/A326S and R178M/A326S, had very low basal steady-state GTPase activities that became demonstrably higher in the presence of RGS4 (*e.g.*, Fig. 4A–B); the GAP effect on $G\alpha_{i1}$(R178M/A326S) was greater than with the $G\alpha_{i1}$(R178C/A326S) variant (GAP factors of 6.5 and 3.6, respectively; Fig. 4E). Given its high GAP factor response in both the steady-state [γ-^{32}P]GTP hydrolysis assay (Fig. 2) and the Transcreener GDP assay (Fig. 4), the $G\alpha_{i1}$(R178M/A326S) variant was used in subsequent analyses.

$G\alpha_{i1}$(R178M/A326S) interacts with RGS proteins with same affinity and specificity as wildtype

A possible concern about the use of a mutated Gα protein for RGS protein GAP assays is that the mutation(s) could disrupt the global fold of Gα or, at the very least, affect the disposition of the switch regions and other surface contact points to which RGS proteins interact 24,31, thereby altering the normal affinity and specificity that RGS proteins show for their various Gα substrates. The two point mutations of R178M and A326S are interior

to the guanine nucleotide binding pocket (Figure 5), but could nevertheless affect the RGS domain interaction surface.

To test for this possibility, we used SPR to compare the binding interactions of RGS2 and RGS16 with wildtype $G\alpha_{i1}$ *versus* the $G\alpha_{i1}$(R178M/A326S) variant. Multiple previous studies 8,24,32 have established that RGS2, a potent GAP for $G\alpha_q$, does not interact with wildtype $G\alpha_{i1}$ *in vitro*; this same lack of interaction was observed with the $G\alpha_{i1}$(R178M/A326S) mutant (data not shown). Conversely, RGS16 is known to be a $G\alpha_i$-interacting RGS protein 24, and was found by SPR to bind equivalently to immobilized wildtype $G\alpha_{i1}$ and $G\alpha_{i1}$(R178M/A326S) proteins (Fig. 6). This equivalence included RGS16 only interacting with high affinity to the Gα subunits in their transition state-mimetic form (namely, Gα in complex with GDP and aluminum tetrafluoride 31). These binding results suggest that no long-range perturbations have been made to the RGS domain interaction sites on $G\alpha_{i1}$ by the two rate-altering mutations of R178M and A326S.

Using the Transcreener GDP assay, we performed an additional test of the $G\alpha_{i1}$(R178M/A326S) variant to control for any unintended changes the two point mutations could have engendered within Gα to alter its interaction specificity with various RGS proteins. With the same RGS protein spectrum used in the SPR binding experiments, we found that RGS2 (highly selective for $G\alpha_q$ over $G\alpha_i$ substrates) had no effect on increasing steady-state GTPase activity of $G\alpha_{i1}$(R178M/A326S), whereas RGS16 increased steady-state GTPase activity 12-fold over the basal rate (Fig. 7).

Pilot screen for inhibitors of RGS4 GAP activity on $G\alpha_{i1}$(R178M/A326S)

Given the robust performance of the Transcreener GDP assay in the control screen for potential compound interference (Fig. 3D) and evidence that the two mutations to $G\alpha_{i1}$ affected neither the affinity nor specificity of the Gα/RGS domain interaction (Figs. 6 and 7), we proceeded to a pilot screen with $G\alpha_{i1}$(R178M/A326S) and RGS4 using the GenPlus library of 960 bioactive molecules (Fig. 8). The screening window was first optimized by varying the concentrations of Gα and RGS protein inputs; at 50 nM $G\alpha_{i1}$(R178M/A326S) and 250 nM RGS4, a maximal signal to background difference of 112 mP units was obtained after 120 minutes of elapsed reaction time before FP measurement. The thiol-reactive compound CCG-4986 was used in the screen as a positive control for RGS4 inhibition 13,33. The GenPlus library screen was conducted with $G\alpha_{i1}$(R178M/A326S) and RGS4 (Fig. 8A); a separate counterscreen of the library was performed with $G\alpha_{i1}$(R178M/A326S) and no RGS4 (Fig. 8B) to identify compounds having either non-specific effects or modifying $G\alpha_{i1}$ GTPase activity (rather than RGS4 GAP activity *per se*).

Z'-factors of 0.60, 0.83, 0.83, and 0.82 were obtained at 60, 90, 120, and 180 minutes elapsed reaction time, as calculated based on data from control wells containing either $G\alpha_{i1}$(R178M/A326S) only or $G\alpha_{i1}$(R178M/A326S) plus RGS4. Note that these Z'-factor values reflect only the RGS4-dependent increase in GTPase activity, and not the total observed GTPase activity relative to no-enzyme controls. The Z-factor for the GenPlus library screen at the 120 minute time point (shown in Fig. 8A) was 0.73, which was calculated by excluding values from wells containing hit compounds. Of the 960 compounds in the GenPlus library, 17 compounds were initially considered hits in the RGS4/Gα screen: *i.e.*, those data points that fell outside the $\mu \pm 3\sigma$ range. However, ten of these 17 hits also resulted in a greater than $\pm 3\sigma$ change in the mean signal within the Gα-only counterscreen and thus were excluded because these compounds are likely either affecting the Gα subunit or otherwise interfering with the assay. Thus the RGS4-specific hit rate was 0.7%: seven compounds from the 960 compound library exhibited an modulatory effect on GDP production that was specific to RGS4-stimulated GTPase activity (Fig. 8A *vs* 8B). Six compounds (id # 62, 63, 244, 413, 524, 812) exhibited an RGS4-specific inhibitory effect

(*i.e.*, a change in polarization greater than the [mean + 3 S.D.] signal threshold) and one compound (#596) exhibited an RGS4-specific activating effect on GDP production (*i.e.*, a change in polarization less than the [mean − 3 S.D.] signal threshold). This hit rate may be artificially high in this pilot screen given that the collection of compounds surveyed (GenPlus library) is not a diverse sampling of chemical space but a collection of US, European, and Japanese approved drugs and other bioactive compounds. As expected 13,33, the thiol-reactive RGS4 inhibitor CCG-4986 consistently exhibited inhibition of RGS4-stimulated GDP production (Fig. 8A).

To our knowledge, the combined use of a GDP detection assay with a rate-altered Gα subunit represents a unique strategy to the detection of RGS protein GAP activity. Even though the two primary components of Gα catalysis, GTP hydrolysis rate and product release, were altered significantly by mutation, the resultant Gα subunits still served as functional substrates for the GTPase-accelerating activity of RGS proteins. Using this double mutation strategy to develop a steady-state RGS protein GAP assay that is easy for the non-specialist to perform, and is well-suited for HTS, removes a major technical barrier preventing the exploration of RGS proteins as therapeutic targets. Moreover, $G\alpha_{i1}$ is a substrate for the GAP activity of several RGS protein family members 24 in addition to those we have tested here; thus, the reagents and methods that we have described should have broad applicability across the protein family. Employing the rate-altered $G\alpha_{i1}$(R178M/A326S) mutant in a homogeneous, end-point-based, enzymatic HTS assay will not only be useful in screening for RGS protein inhibitors but, unlike existing assays based on the RGS domain/Gα binding interaction 11−13, this enzymatic assay should also facilitate identification of small molecule *activators* of RGS domain-mediated GAP activity. The lipid moiety phosphatidylinositol-3,4,5-trisphophate (PIP_3) has been shown to bind to, and thereby inhibit in an allosteric fashion, the GAP activity of select RGS domains such as that of RGS4 23; Ca^{2+}/calmodulin reverses this PIP_3-mediated inhibition by competing for the PIP_3-binding site 23. A small molecule targeting this site of allosteric modulation over RGS domain GAP activity could potentially be quite valuable therapeutically in pathophysiological situations which may arise from a loss of RGS protein activity, such as RGS2 in hypertension 34 and RGS4 in schizophrenia 35.

Acknowledgments

Thanks to Drs. Christopher Johnston and Francis Willard (UNC) for initial discussions regarding rate-altering Gα mutations, and Dr. Steve Hayes (BellBrook Labs) for discussion and critical appraisal of the manuscript. Work at BellBrook Labs was supported by NIH SBIR grant R43 NS059082 and work in the Siderovski lab was funded by NIH grant R01 GM082892. A.J.K. acknowledges early support from NIH training grant T32 GM008719 and current support from NIH fellowship F30 MH074266.

REFERENCES

1. Gilman AG. G proteins: transducers of receptor-generated signals. Annu Rev Biochem. 1987; 56:615–649. [PubMed: 3113327]
2. McCudden CR, Hains MD, Kimple RJ, Siderovski DP, Willard FS. G-protein signaling: back to the future. Cell Mol Life Sci. 2005; 62:551–577. [PubMed: 15747061]
3. Siderovski DP, Hessel A, Chung S, Mak TW, Tyers M. A new family of regulators of G-protein-coupled receptors? Curr Biol. 1996; 6:211–212. [PubMed: 8673468]
4. Koelle MR, Horvitz HR. EGL-10 regulates G protein signaling in the C. elegans nervous system and shares a conserved domain with many mammalian proteins. Cell. 1996; 84:115–125. [PubMed: 8548815]
5. Druey KM, Blumer KJ, Kang VH, Kehrl JH. Inhibition of G-protein-mediated MAP kinase activation by a new mammalian gene family. Nature. 1996; 379:742–746. [PubMed: 8602223]

6. Berman DM, Wilkie TM, Gilman AG. GAIP and RGS4 are GTPase-activating proteins for the Gi subfamily of G protein alpha subunits. Cell. 1996; 86:445–452. [PubMed: 8756726]
7. Neubig RR, Siderovski DP. Regulators of G-protein signalling as new central nervous system drug targets. Nat Rev Drug Discov. 2002; 1:187–197. [PubMed: 12120503]
8. Ingi T, Krumins AM, Chidiac P, Brothers GM, Chung S, Snow BE, Barnes CA, Lanahan AA, Siderovski DP, Ross EM, Gilman AG, Worley PF. Dynamic regulation of RGS2 suggests a novel mechanism in G-protein signaling and neuronal plasticity. J Neurosci. 1998; 18:7178–7188. [PubMed: 9736641]
9. Ross EM. Quantitative assays for GTPase-activating proteins. Methods Enzymol. 2002; 344:601–617. [PubMed: 11771414]
10. Willard FS, Siderovski DP. Purification and in vitro functional analysis of the Arabidopsis thaliana regulator of G-protein signaling-1. Methods Enzymol. 2004; 389:320–338. [PubMed: 15313574]
11. Willard FS, Kimple RJ, Kimple AJ, Johnston CA, Siderovski DP. Fluorescence-based assays for RGS box function. Methods Enzymol. 2004; 389:56–71. [PubMed: 15313559]
12. Willard FS, Kimple AJ, Johnston CA, Siderovski DP. A direct fluorescence-based assay for RGS domain GTPase accelerating activity. Anal Biochem. 2005; 340:341–351. [PubMed: 15840508]
13. Roman DL, Talbot JN, Roof RA, Sunahara RK, Traynor JR, Neubig RR. Identification of small-molecule inhibitors of RGS4 using a high-throughput flow cytometry protein interaction assay. Mol Pharmacol. 2007; 71:169–175. [PubMed: 17012620]
14. Sondek J, Lambright DG, Noel JP, Hamm HE, Sigler PB. GTPase mechanism of Gproteins from the 1.7-A crystal structure of transducin alpha-GDP-AIF-4. Nature. 1994; 372:276–279. [PubMed: 7969474]
15. Coleman DE, Berghuis AM, Lee E, Linder ME, Gilman AG, Sprang SR. Structures of active conformations of Gi alpha 1 and the mechanism of GTP hydrolysis. Science. 1994; 265:1405–1412. [PubMed: 8073283]
16. Posner BA, Mixon MB, Wall MA, Sprang SR, Gilman AG. The A326S mutant of Gialpha1 as an approximation of the receptor-bound state. J Biol Chem. 1998; 273:21752–21758. [PubMed: 9705312]
17. Nishina H, Nimota K, Kukimoto I, Maehama T, Takahashi K, Hoshino S, Kanaho Y, Katada T. Significance of Thr182 in the nucleotide-exchange and GTP-hydrolysis reactions of the alpha subunit of GTP-binding protein Gi2. J Biochem (Tokyo). 1995; 118:1083–1089. [PubMed: 8749330]
18. Marin EP, Krishna AG, Sakmar TP. Rapid activation of transducin by mutations distant from the nucleotide-binding site: evidence for a mechanistic model of receptor-catalyzed nucleotide exchange by G proteins. J Biol Chem. 2001; 276:27400–27405. [PubMed: 11356823]
19. Kleman-Leyer KM, Klink TA, Kopp AL, Westermeyer TA, Koeff MD, Larson BR, Worzella TJ, van de Kar SAT, Zaman GJR, Hornberg JJ, Lowery RG. Characterization and Optimization of a Red-shifted Fluorescence Polarization ADP Detection Assay. Assay and Drug Development Technologies. 2009; 7:56–67. [PubMed: 19187009]
20. Huss KL, Blonigen PE, Campbell RM. Development of a Transcreener kinase assay for protein kinase A and demonstration of concordance of data with a filter-binding assay format. J Biomol Screen. 2007; 12:578–584. [PubMed: 17409274]
21. Klink TA, Kleman-Leyer KM, Kopp A, Westermeyer TA, Lowery RG. Evaluating PI3 kinase isoforms using Transcreener ADP assays. J Biomol Screen. 2008; 13:476–485. [PubMed: 18566477]
22. Liu Y, Zalameda L, Kim KW, Wang M, McCarter JD. Discovery of acetyl-coenzyme A carboxylase 2 inhibitors: comparison of a fluorescence intensity-based phosphate assay and a fluorescence polarization-based ADP Assay for high-throughput screening. Assay Drug Dev Technol. 2007; 5:225–235. [PubMed: 17477831]
23. Popov SG, Krishna UM, Falck JR, Wilkie TM. Ca2+/Calmodulin reverses phosphatidylinositol 3,4, 5-trisphosphate-dependent inhibition of regulators of G protein-signaling GTPase-activating protein activity. J Biol Chem. 2000; 275:18962–18968. [PubMed: 10747990]
24. Soundararajan M, Willard FS, Kimple AJ, Turnbull AP, Ball LJ, Schoch GA, Gileadi C, Fedorov OY, Dowler EF, Higman VA, Hutsell SQ, Sundstrom M, Doyle DA, Siderovski DP. Structural

diversity in the RGS domain and its interaction with heterotrimeric G protein alpha-subunits. Proc Natl Acad Sci U S A. 2008; 105:6457–6462. [PubMed: 18434541]

25. Johnston CA, Lobanova ES, Shavkunov AS, Low J, Ramer JK, Blaesius R, Fredericks Z, Willard FS, Kuhlman B, Arshavsky VY, Siderovski DP. Minimal determinants for binding activated G alpha from the structure of a G alpha(i1)-peptide dimer. Biochemistry. 2006; 45:11390–11400. [PubMed: 16981699]
26. Afshar K, Willard FS, Colombo K, Johnston CA, McCudden CR, Siderovski DP, Gonczy P. RIC-8 is required for GPR-1/2-dependent Galpha function during asymmetric division of C. elegans embryos. Cell. 2004; 119:219–230. [PubMed: 15479639]
27. Willard FS, Siderovski DP. Covalent immobilization of histidine-tagged proteins for surface plasmon resonance. Anal Biochem. 2006; 353:147–149. [PubMed: 16620750]
28. Ferguson KM, Higashijima T, Smigel MD, Gilman AG. The influence of bound GDP on the kinetics of guanine nucleotide binding to G proteins. J Biol Chem. 1986; 261:7393–7399. [PubMed: 3086311]
29. Lowery RG, Kleman-Leyer K. Transcreener: screening enzymes involved in covalent regulation. Expert Opin Ther Targets. 2006; 10:179–190. [PubMed: 16441236]
30. Zhang JH, Chung TD, Oldenburg KR. A Simple Statistical Parameter for Use in Evaluation and Validation of High Throughput Screening Assays. J Biomol Screen. 1999; 4:67–73. [PubMed: 10838414]
31. Tesmer JJ, Berman DM, Gilman AG, Sprang SR. Structure of RGS4 bound to AlF4--activated G(i alpha1): stabilization of the transition state for GTP hydrolysis. Cell. 1997; 89:251–261. [PubMed: 9108480]
32. Heximer SP, Watson N, Linder ME, Blumer KJ, Hepler JR. RGS2/G0S8 is a selective inhibitor of Gqalpha function. Proc Natl Acad Sci U S A. 1997; 94:14389–14393. [PubMed: 9405622]
33. Kimple AJ, Willard FS, Giguere PM, Johnston CA, Mocanu V, Siderovski DP. The RGS protein inhibitor CCG-4986 is a covalent modifier of the RGS4 Galpha-interaction face. Biochim Biophys Acta. 2007; 1774:1213–1220. [PubMed: 17660054]
34. Heximer SP, Knutsen RH, Sun X, Kaltenbronn KM, Rhee MH, Peng N, Oliveira-dos-Santos A, Penninger JM, Muslin AJ, Steinberg TH, Wyss JM, Mecham RP, Blumer KJ. Hypertension and prolonged vasoconstrictor signaling in RGS2-deficient mice. J Clin Invest. 2003; 111:445–452. [PubMed: 12588882]
35. Mirnics K, Middleton FA, Stanwood GD, Lewis DA, Levitt P. Disease-specific changes in regulator of G-protein signaling 4 (RGS4) expression in schizophrenia. Mol Psychiatry. 2001; 6:293–301. [PubMed: 11326297]

A

Mutation (*ref.*)	Gα protein mutated	Increase in $k_{off(GDP)}$	Decrease in $k_{cat(GTPase)}$	Equivalent site in $G\alpha_{i1}$	RGS protein interaction?
A326S (*16*)	$G\alpha_{i1}$	25x	none	A326	RGS4
R178C (*15*)	$G\alpha_{i1}$	Reported, not quantified	>100x	R178	RGS4
T182A (*17*)	$G\alpha_{i2}$	2x	>100x	T181	n.d.
K188A (*18*)	$G\alpha_{t}$	6x	n.d.	K192	n.d.
F332A (*18*)	$G\alpha_{t}$	>150x	n.d.	F336	n.d.

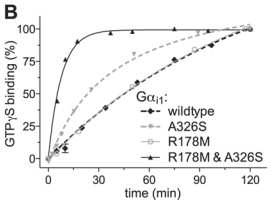

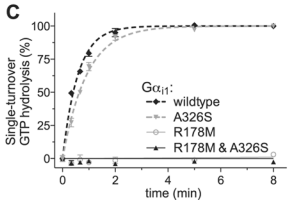

D

$G\alpha_{i1}$ species:	GTP binding (min^{-1})	GTP hydrolysis (min^{-1})
wildtype	0.009	1.7
A326S	0.027	1.1
R178M	0.008	0.001
R178C	0.009	0.008
R178C/ A326S	0.025	0.000
R178M/ A236S	0.130	0.000

Figure 1. Increased GDP release and decreased GTP hydrolysis of the $G\alpha_{i1}$(R178M/A326S) mutant compared to wildtype $G\alpha_{i1}$ and single point-mutants, as measured by [^{35}S]GTPγS binding and single-turnover [γ-^{32}P]GTP hydrolysis, respectively

(A) Point mutations to $G\alpha_i$-family subunits previously reported in the literature 15⁻18 to alter intrinsic GTP hydrolysis and GDP dissociation rates. (**B**) Binding of [^{35}S]GTPγS to wildtype or indicated mutant $G\alpha_{i1}$ subunits. (**C**) Single-turnover GTP hydrolysis activities of wildtype or indicated mutant $G\alpha_{i1}$ subunits. (**D**) Initial rates of GTP binding and hydrolysis for the $G\alpha_{i1}$(R178M/A326S) mutant, as well as other $G\alpha_{i1}$ point mutants derived from data similar to that of panels B and C.

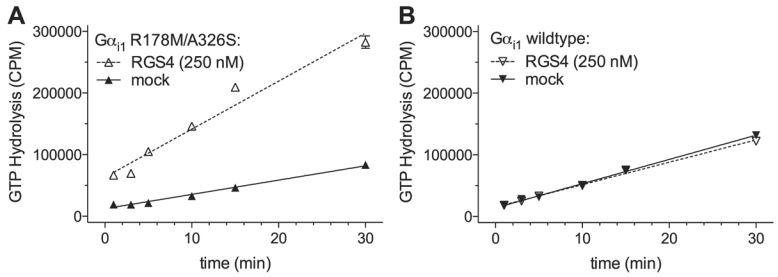

Figure 2. RGS4 GAP activity is observed as an increase in steady-state GTP hydrolysis only for the rate-altered $G\alpha_{i1}$(R178M/A326S) variant

Time courses of steady-state [γ-^{32}P]GTP hydrolysis by 50 nM $G\alpha_{i1}$(R178M/A326S) mutant (A) or 50 nM wildtype $G\alpha_{i1}$ (B) in the presence or absence of 250 nM RGS4 at 20°C. Results are the mean (± S.E.M.) of duplicate samples.

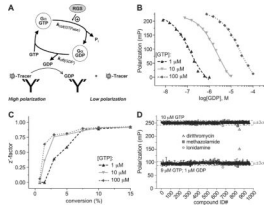

Figure 3. Fluorescence polarization immunoassay for the detection of GDP

(**A**) Schematic representation of methodology underlying the Transcreener GDP assay as applied to steady-state GTP hydrolysis (and resultant GDP production) by a rate-altered Gα protein. Fluorescent tracer is illustrated with a jagged oval; when bound to the GDP-selective monoclonal antibody, emitted light remains polarized, whereas there is low polarization of emitted light when tracer is displaced by free GDP. (**B**) The Transcreener GDP assay was used to generate standard curves for conversion of GTP into GDP at initial GTP concentrations of 1, 10, and 100 μM using appropriate EC_{85} concentrations of GDP antibody established for these initial GTP concentrations (2.2, 12, and 64 μg/mL, respectively). (**C**) Z'-factor values, reflecting both assay signal window and signal variability 30, were determined in 16 replicates for each of the points in the GDP-detection standard curves presented in panel B. Although the assay window was reduced at lower percent conversions (*e.g.*, 57 mP for 3% conversion to GDP of 10 μM initial GTP; panel B), acceptable Z'-factors 30 of >0.5 were observed down to 2% conversion for the two higher initial GTP concentrations and to 5% for the 1 μM initial GTP curve, given the very low signal variability. (**D**) Control screen using the 960 compound GenPlus library. Assay components were added to duplicate wells containing 10 μM compound and either 10 μM GTP (to mimic no-enzyme control reactions) or 9 μM GTP plus 1 μM GTP (to mimic completed GTPase reactions). The range of signal observed (3 standard deviations about the mean; "μ±3σ") in each condition is demarked with a dotted grey line.

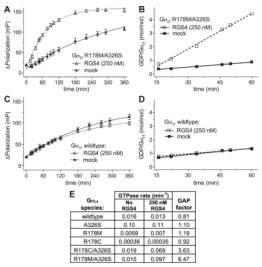

$G\alpha_{i1}$ species:	GTPase rate (min^{-1}) No RGS4	250 nM RGS4	GAP factor
wildtype	0.016	0.013	0.81
A326S	0.10	0.11	1.10
R178M	0.0059	0.007	1.19
R178C	0.00038	0.00035	0.92
R178C/A326S	0.019	0.069	3.63
R178M/A326S	0.015	0.097	6.47

Figure 4. RGS4 increases the steady-state GTPase activity of $G\alpha_{i1}$(R178M/A326S) but not wildtype $G\alpha_{i1}$, as measured using the Transcreener GDP assay and reported in absolute change in polarization (*left panels*) and GDP produced per G*α* protein in reaction (*right panels*)

R178M/A326S double-mutant (**A,B**) and wildtype (**C,D**) $G\alpha_{i1}$ proteins were present at 50 nM final concentration. Dashed lines represent reactions conducted in the presence, and solid lines ("mock") in the absence, of 250 nM RGS4 protein. (**A,C**) Change in polarization (ΔmP) at each time-point for indicated $G\alpha_{i1}$ protein was calculated as $\Delta mP = |mP(G\alpha_{i1}) - mP(\text{no } G\alpha_{i1})|$. (**B,D**) Data from panels A and C were converted to GDP produced per mol of input $G\alpha_{i1}$ using previously established standard curves for GDP detection in the presence of GTP (*e.g.*, Figure 3B). (**E**) Summary of initial rates obtained by the Transcreener GDP assay for each $G\alpha_{i1}$ mutant tested. "GAP factor" is defined as the ratio between steady-state GTPase rate in the presence of RGS protein and steady-state GTPase rate in the absence of RGS protein.

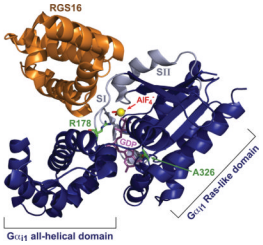

Figure 5. Structural features of the RGS16/Gα_{i1}·GDP·AlF $^{-}_{4}$ complex highlighting the locations of Arg-178 and Ala-326 residue positions mutated in the Gα_{i1}(R178M/A326S) variant

The RGS16/Gα complex (PDB id 2IK8; ref. 24), was rendered using PyMOL with the RGS16 RGS domain in *orange* and Gα_{i1} protein in *blue*, respectively. Gα_{i1} switch regions are depicted in *grey*; switches one and two (SI, SII) are visible in the foreground, whereas switch three is in the background and thus unlabeled. GDP is shown in *magenta*, the AlF $^{-}_{4}$ ion is *red*, and Mg^{2+} ion is depicted as a *yellow* sphere. Residues arginine-178 and alanine-326 are rendered as `sticks' in *green* with CPK atomic coloring (nitrogen = *blue*, oxygen = *red*).

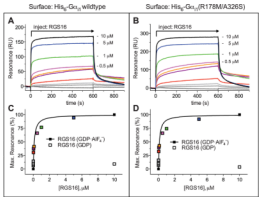

Figure 6. RGS16 binds equivalently to wildtype $G\alpha_{i1}$ and the rate-altered G α_{i1} (R178M/A326S) mutant

(**A,B**) Sensorgrams derived from 600 second injections of various concentrations (3 nM to 10 μM) of RGS16 over SPR biosensors of immobilized (**A**) wildtype $G\alpha_{i1}$·GDP·AlF^{-}_{4} or (**B**) $G\alpha_{i1}$(R178M/A326S)·GDP·$AlF^{\ddagger}_{4}$. SPR experiments were also conducted with both $G\alpha_{i1}$ subunits in their inactive, GDP-bound state (data not shown). (**C,D**) Resultant sensorgrams were used in equilibrium saturation binding analyses (as previously described 24) to derive dissociation constants (K_D values). RGS16 bound to wildtype $G\alpha_{i1}$·GDP·AlF^{-}_{4} with a dissociation constant of 124 nM (95% C.I. of 76–174 nM; panel **C**), whereas RGS16 bound to $G\alpha_{i1}$(R178M/A326S)·GDP·AlF^{-}_{4} with a dissociation constant of 115 nM (64–166 nM; panel **D**). Note that interactions were not observed (for either Gα subunit) when the Gα was GDP-bound (as expected; refs. 24,31), nor when RGS2 was injected (data not shown).

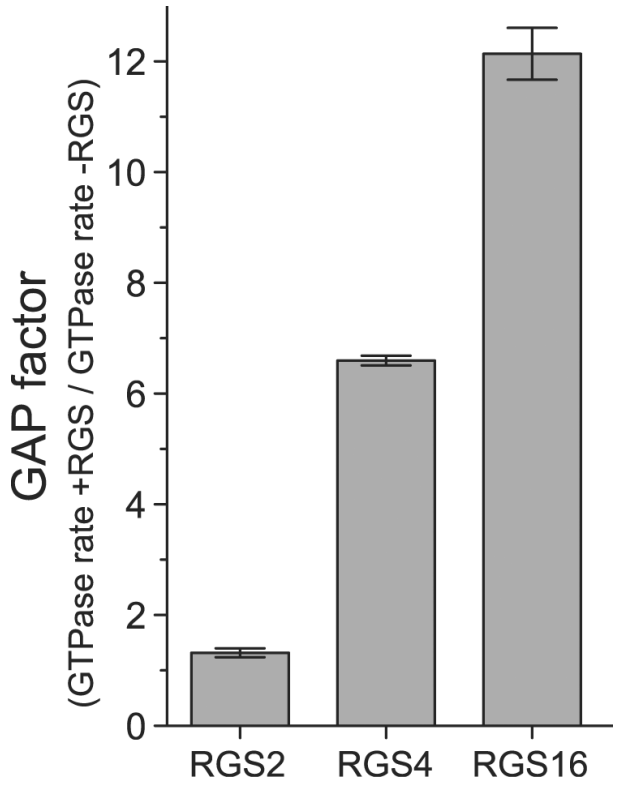

Figure 7. The steady-state GTPase activity of $G\alpha_{i1}$(R178M/A326S) is increased by RGS4 and RGS16, but not by the $G\alpha_q$-selective RGS2

Transcreener GDP assays were performed as in Figure 4, using 250 nM of the indicated RGS protein. Moles of GDP produced per mol input $G\alpha_{i1}$(R178M/A326S) protein were first plotted over time using GraphPad Prism and linear regression performed to determine steady-state GTPase rates. Presented bar graph denotes GAP factors derived from these steady-state GTPase rates.

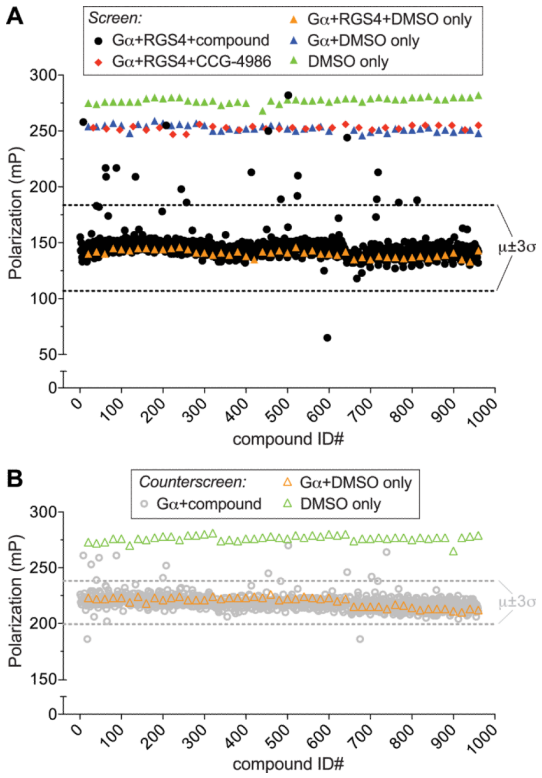

Figure 8. Pilot screen and counterscreen using the 960 compound GenPlus library

Transcreener GDP assay components were added to wells containing 50 nM $G\alpha_{i1}$ (R178M/A326S) with (panel **A**) or without (panel **B**) 250 nM RGS4 protein and either 10 μM compound (in 0.5% [v/v] final concentration of DMSO), 150 μM of reactive RGS4 inhibitor CCG-4986, or 0.5% DMSO only, as indicated in the legends. The range of signal observed (three standard deviations [σ] about the mean [μ]) is denoted by the dashed lines for the 960 compound library screen using RGS4 and $G\alpha_{i1}$ (R178M/A326S) (*black;* panel **A**, coefficient of variation [CV%] = 8.8%) and library counterscreen using $G\alpha_{i1}$ (R178M/A326S) alone (*gray;* panel **B**, CV% = 3.0%). Data in panel **A** was obtained at 120 minutes of elapsed reaction time; data in panel **B** was obtained after 210 minutes of elapsed reaction time, given the slower GTPase (and GDP production) rate of $G\alpha_{i1}$ (R178M/A326S) in the absence of RGS4 GAP activity.